Empirical relationship between entrainment rate and microphysics in cumulus clouds

Chunsong Lu,[1,2] Shengjie Niu,[1] Yangang Liu,[2] and Andrew M. Vogelmann[2]

Received 16 March 2013; accepted 3 April 2013; published 22 May 2013.

[1] The relationships between fractional entrainment rate and key microphysical quantities (e.g., liquid water content, droplet number concentration, volume mean radius, and standard deviation of cloud droplet size distributions) in shallow cumuli are empirically examined using in situ aircraft observations from the Routine Atmospheric Radiation Measurement Aerial Facility Clouds with Low Optical Water Depths Optical Radiative Observations (RACORO) field campaign over the Atmospheric Radiation Measurement Southern Great Plains site. The results show that the microphysical quantities examined generally exhibit strong relationships with entrainment rate and that the relationships collectively suggest the dominance of homogeneous entrainment mixing, which is unfavorable to the formation of large droplets and the initiation of warm rain in the clouds. The dominance of the homogeneous mixing mechanism is further substantiated by the dependency on entrainment rate of relationships among various microphysical variables and of cloud droplet size distributions. The dominance of this mechanism is also quantitatively confirmed by examining the degree of homogeneous mixing in the clouds. The dominance of homogeneous mixing may be an important reason why none of the cumulus clouds studied was drizzling.
Citation: Lu, C., S. Niu, Y. Liu, and A. M. Vogelmann (2013), Empirical relationship between entrainment rate and microphysics in cumulus clouds, *Geophys. Res. Lett.*, *40*, 2333–2338, doi:10.1002/grl.50445.

1. Introduction

[2] Turbulent entrainment mixing processes have been thought to be likely candidates for resolving some prominent problems in cloud physics (e.g., warm rain initiation) since the late 1940s [*Stommel*, 1947; *Su et al*., 1998; *Lasher-Trapp et al*., 2005]. The need for improving the understanding of entrainment mixing processes is further reinforced by the growing interest in aerosol indirect effects and cloud-climate feedbacks [e.g., *Hill et al*., 2009].

[3] One important topic concerning entrainment mixing processes is the fractional entrainment rate (λ), which affects the interaction between clouds and their environments [*Sanderson et al*., 2008; *Romps*, 2010]. Recently, using the approach presented by *Lu et al*. [2012b], *Lu et al*. [2012a] estimated λ in eight cumulus flights during the Routine AAF [Atmospheric Radiation Measurement (ARM) Aerial Facility] Clouds with Low Optical Water Depths (CLOWD) Optical Radiative Observations (RACORO) field campaign, which operated over the ARM Southern Great Plains site near Lamont, Oklahoma, from 22 January to 30 June 2009 [*Vogelmann et al*., 2012].

[4] Besides entrainment rate, entrainment mixing mechanisms and their influences on cloud microphysics are also a topic of intensive research and debate [*Baker et al*., 1980; *Gerber et al*., 2008; *Lu et al*., 2011]. Some studies suggest that the entrainment mixing process is close to being homogeneous [e.g., *Jensen et al*., 1985], others suggest that the mixing is extremely inhomogeneous [e.g., *Freud et al*., 2011], and still others suggest that the mechanism is neither homogeneous nor extremely inhomogeneous [*Lehmann et al*., 2009; *Lu et al*., 2013b]. In particular, the relationship between entrainment rate and cloud microphysics remains underexplored, due mainly to the lack of simultaneous measurements of cloud microphysical properties and entrainment rate. This paper addresses a significant gap in the understanding of entrainment mixing processes and their interactions with cloud microphysics by analyzing microphysical measurements with entrainment rates that were derived for RACORO cumulus clouds. Examined are the influences of entrainment rate on microphysical properties, microphysical relationships, and droplet size distributions. The results are further inspected in the context of a recently proposed measure of homogeneous mixing degree [*Lu et al*., 2013b].

2. RACORO Data and Approach

2.1. RACORO Data

[5] During RACORO, the Center for Interdisciplinary Remotely Piloted Aircraft Studies (CIRPAS) Twin Otter aircraft made comprehensive measurements of cloud, aerosol, radiation, and atmospheric state parameters. The aircraft flew at multiple levels to measure cloud droplet size distributions in different clouds using a cloud and aerosol spectrometer (CAS) at a 10 Hz sampling rate. The CAS probe sizes and counts aerosol particles and cloud droplets from 0.29 to 25 μm (radius) in 20 bins. Here only the droplets with a bin-average radius larger than 1 μm are used to calculate cloud microphysical properties [e.g., liquid water content (LWC)]. The radius of ~1 μm is often taken as the lower limit of cloud droplets in the literature [e.g., *Deng*

[1]Key Laboratory of Meteorological Disaster of Ministry of Education, Key Laboratory for Aerosol-Cloud-Precipitation of China Meteorological Administration, Nanjing University of Information Science and Technology, Jiangsu, China.
[2]Atmospheric Sciences Division, Brookhaven National Laboratory, Upton, New York, USA.

Corresponding author: C. Lu, Key Laboratory of Meteorological Disaster of Ministry of Education, Key Laboratory for Aerosol-Cloud-Precipitation of China Meteorological Administration, Nanjing University of Information Science and Technology, Room 1005, Qixiang Bldg., No. 219, Ningliu Rd., Pukou, Nanjing, Jiangsu 210044, China. (luchunsong110@gmail.com)

0094-8276/13/10.1002/grl.50445

et al., 2009]. The cloud imaging probe (CIP) measured droplets in the range of 7.5 to 781 μm (radius) at 1 Hz. Temperature and water vapor concentration were measured at 10 Hz, respectively, with a Rosemount probe and a diode laser hygrometer [*Diskin et al*., 2002]. Cloud droplet size distributions with a droplet number concentration (N) $>10\,\mathrm{cm}^{-3}$ and an LWC $>0.001\,\mathrm{g\,m}^{-3}$ are considered to be cloud records [e.g., *Deng et al*., 2009]. Non-drizzling clouds in a flight must further satisfy the condition that the in-cloud mean drizzle LWC (drop radius >25 μm) from the CIP over the observation period of the flight was smaller than $0.005\,\mathrm{g\,m}^{-3}$. All the cumulus clouds analyzed were not drizzling.

2.2. Approach for Estimating Entrainment Rate

[6] *Lu et al*. [2012a] estimated λ in 186 growing cumulus cloud cores during eight RACORO flights. Only one penetration level was used for each cloud. Growing cumulus clouds in these flights were selected based on the following criteria: (1) 80% of vertical velocity (w) in an individual cloud is positive [*Gerber et al*., 2008; *Lu et al*., 2012b] and (2) the number of cloud droplet size distributions is higher than 30 to select relatively large cumulus clouds. The edge of the cloud core is defined as the point going from the cloud edge toward the cloud interior where vertical velocity changes from negative to positive for the first time (see Figure 1 in the work of *Lu et al*. [2012a] for details).

[7] The approach for estimating λ was developed by *Lu et al*. [2012b] (see Auxiliary Material for details). First, the dry air at the aircraft penetration level (z) is assumed to be entrained into the adiabatic cloud at that level and the dilution of the cloud, which is represented by the mixing fraction of adiabatic cloud (χ), is determined. This assumption is widely used [e.g., *Gerber et al*., 2008]. The estimation of χ uses the equations for the conservation of total water and energy during the mixing at z. The adiabatic liquid water mixing ratio (q_{La}) is needed, and it is derived from adiabatic LWC ($\mathrm{LWC_a}$). $\mathrm{LWC_a}$ is assumed to be the maximum LWC in a cloud. The water vapor mixing ratio corresponding to $\mathrm{LWC_a}$ is taken as the water vapor mixing ratio in the adiabatic cloud [q_{vs} (T_{a})], and the temperature (T_{a}) in the adiabatic cloud is calculated from q_{vs} assuming saturation in the adiabatic cloud. Second, the cloud base height (z_0) is estimated by adiabatic extrapolation to the height of $\mathrm{LWC_a}=0$; the height (h) of the penetration level above z_0 is $z-z_0$. Third, although the entrained dry air is assumed from environmental air at the observation level to calculate χ, in reality, the entrainment processes responsible for the dilution of the cloud may occur not only at the penetration level but also at several levels or even continuously from z_0 to z. Therefore, it is more reasonable to calculate the average entrainment rate from z_0 to z by

$$\lambda = \frac{-\ln\chi}{h}. \tag{1}$$

[8] Three points are worth noting. First, the assumed $\mathrm{LWC_a}$ along a leg might be less than the true $\mathrm{LWC_a}$ due to inherent spatial averaging of the sampling probe and possible influences of entrainment mixing processes. Within a distance of ~5 m (sampling rate of 10 Hz and aircraft speed of $\sim 50\,\mathrm{m\,s}^{-1}$), the CAS probe might encounter some cloud areas diluted by entrained environmental air. The error in $\mathrm{LWC_a}$, if any, will affect the estimated cloud base height and h. Second, other approaches for estimating cloud base height and $\mathrm{LWC_a}$ have been reported in the literature. For example, a cloud base height for a flight may be estimated using temperature and moisture from surface stations, estimated from aircraft flights in the dry boundary layer, or obtained from some direct (e.g., lidar) measurements [e.g., *Clothiaux et al*., 2000]. A cloud base height may also be obtained by fitting peak LWC values at different observation levels with a linear profile [e.g., *Gerber et al*., 2008]. Knowing the cloud base height, $\mathrm{LWC_a}$ can be calculated. Unfortunately, none of these approaches is applicable here because cloud base heights varied significantly during flights in RACORO [*Vogelmann et al*., 2012], making it inappropriate to assume a constant cloud base height for different clouds during a flight. In addition, time is needed for the aircraft to change its altitude and, during that time, the properties of the shallow cumuli may change. Therefore, instead, an entrainment rate value is estimated for each individual cloud. Third, with the potential errors in estimated $\mathrm{LWC_a}$, cloud base heights, and h in mind, their effects on the estimated λ are likely small because of the cancellation of effects on h and χ in equation (1). An uncertainty analysis shows that increasing the true $\mathrm{LWC_a}$ by 25% results in an increase in the estimated entrainment rate of 10% to 16%, depending on the source of entrained dry air [*Lu et al*. [2012a] (see section 3 for a discussion of dry air sources).

3. Observational Relationships Between Entrainment Rate and Microphysics

[9] As mentioned above, in the work of *Lu et al*. [2012a], the average λ was calculated for each cloud core of 186 growing cumulus clouds for different D values, where the dry air was assumed to be entrained from the air that is D to $2D$ from the edge of a cloud core on both sides of an aircraft's cloud penetration. D can be thought of representing the size of a grid cell within a high-resolution model, and D was set to be 10, 20, 30, 40, 50, 100, 300, and 500 m (see *Lu et al*. [2012a, 2012b] for more explanations on D and the calculation of λ). The same data set of λ is used here to examine the effects of λ on cloud microphysical variables and their relationships as well as on cloud droplet size distributions.

[10] Figure 1 shows the relationships of λ with LWC, N, and the droplet size distribution's standard deviation (σ), mean radius (r_{m}), volume mean radius (r_{v}), and relative dispersion (d, the ratio of σ to r_{m}). Note that the results shown here are for $D=50$ m; the results for other values of D are similar. The wide spread of entrainment rate from ~0.1 to $\sim 10\,\mathrm{km}^{-1}$ is caused by the vertical variation of entrainment rate and the large standard deviation of entrainment rate at lower levels in clouds (see Auxiliary Material for details). The negative correlations of λ with LWC and with N are consistent with the theoretical expectation that a larger λ indicates stronger dilution and evaporation, causing smaller values of LWC and N. The decrease in droplet size (r_{v} or r_{m}) with increasing λ suggests that the entrainment results in a larger fractional reduction in LWC than in N, according to the equation describing the relationship between r_{v}, LWC, and N ($r_{\mathrm{v}}^3 \sim \mathrm{LWC}/N$). The correlation between λ and d is positive, which is mainly due to the

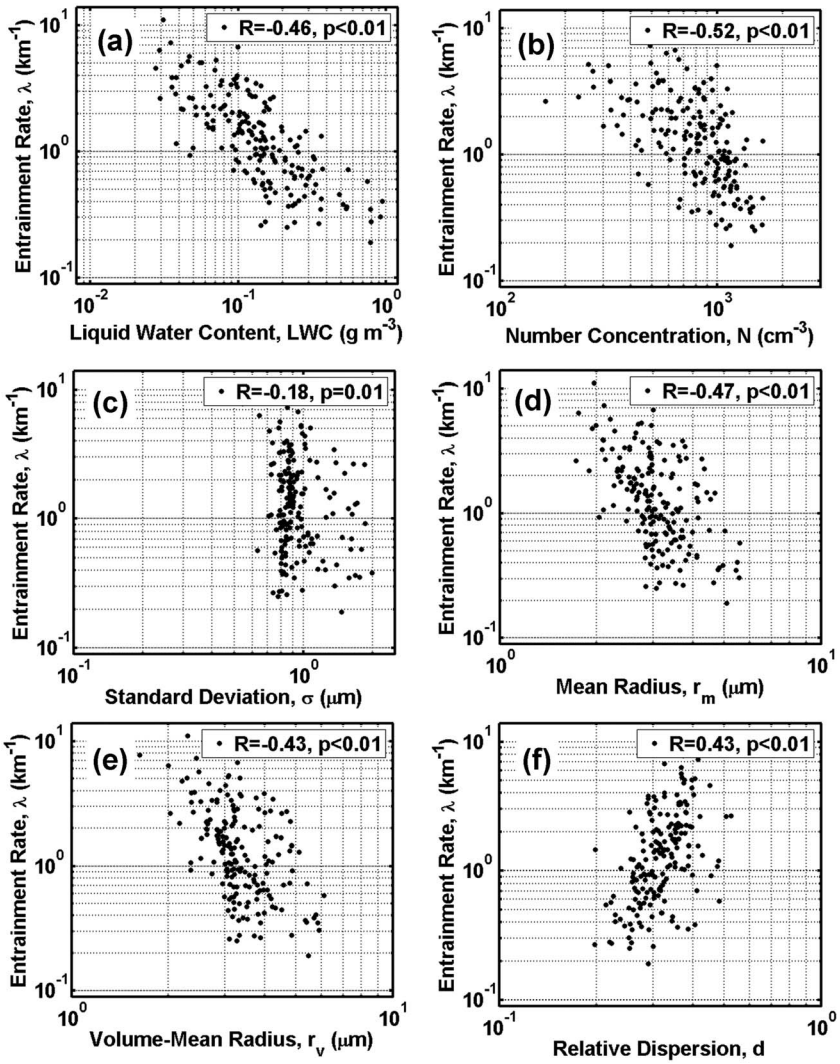

Figure 1. Entrainment rate (λ) as a function of (a) liquid water content (LWC), (b) droplet number concentration (N), and the droplet size distribution's (c) standard deviation (σ), (d) mean radius (r_m), (e) volume mean radius (r_v), and (f) relative dispersion (d) in 186 growing cumulus clouds during RACORO. The entrained dry air is assumed to be from D to $2D$ away (horizontally) from the edge of the cloud core, where here $D = 50$ m. Each legend provides a correlation coefficient (R) and the p value of the correlation.

negative correlation between λ and r_m. The correlation between σ and λ is still negative but with a weak correlation coefficient of -0.18, and σ remains approximately constant between 0.75 and 1 μm. The result of a roughly constant σ is similar to that reported by *Pawlowska et al*. [2006], who found that σ in the marine stratocumulus clouds examined varied little between 1 and 2 μm. Furthermore, the positive λ-d relationship and the negative λ-r_m and λ-r_v relationships together suggest that entrainment mixing processes broaden droplet size distributions toward smaller sizes and thus are not favorable to the production of large droplets that are conducive to warm rain initiation. These results are in qualitative agreement with the homogeneous entrainment mixing theory. The effect of entrainment mixing processes can also be seen in the relationship between λ and the skewness of cloud droplet size distributions (Figure S3 in Auxiliary Material). The relationships between microphysical properties and $1-\mathrm{LWC/LWC_a}$ are also examined (Figure S4 in Auxiliary Material); they are similar to the relationships between microphysical properties and entrainment rate. The similarity between the two sets of relationships suggests that the conclusions obtained from the above analysis with entrainment rate can represent the effects of entrainment mixing processes. Furthermore, the correlation coefficients of the relationships between entrainment rate and LWC, r_m, and r_v are larger than those between $1-\mathrm{LWC/LWC_a}$ and LWC, r_m, and r_v.

[11] As discussed above, the approaches used to estimate $\mathrm{LWC_a}$ and cloud base heights may lead to some errors in estimated λ. To examine how the uncertainty of $\mathrm{LWC_a}$ affects the above relationships, Figure 1 is replotted with λ calculated assuming $\mathrm{LWC_a}$ is 1.25 times the maximum LWC. The result (Figure S5 in Auxiliary Material) shows that the above relationships are almost the same as those shown in Figure 1.

[12] In addition to individual microphysical quantities, their interrelationships often reveal more information on the underlying physics. To quantify the effect of entrainment rate on such relationships, Figure 2 shows the microphysical relationships among LWC, N, d, σ, and r_v that are binned

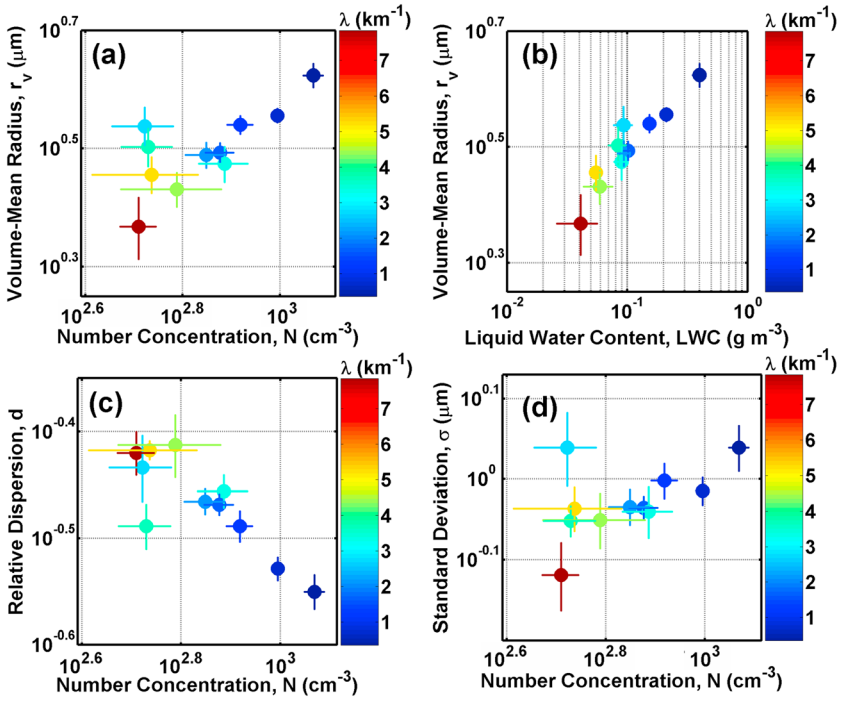

Figure 2. (a) Volume mean radius (r_v) as a function of droplet number concentration (N), (b) r_v as a function of liquid water content (LWC), (c) relative dispersion (d) as a function of N, and (d) standard deviation (σ) as a function of N, which are binned according to entrainment rate (λ) in 186 growing cumulus clouds during RACORO. The bars represent standard errors of the mean for each bin. The entrained dry air is assumed to be from D to $2D$ away (horizontally) from the edge of the cloud core, where here $D = 50$ m.

according to λ. Binning by λ helps reduce the large scatter in Figure 1. The relationships of r_m with other properties are not shown since they are similar to those shown for r_v. The positive correlations of r_v with N and with LWC qualitatively confirm that homogeneous mixing dominates in the shallow cumuli. The correlation between d and N is negative because homogeneous mixing with larger λ increases d and decreases N. As mentioned above, σ is mainly in the narrow range of 0.75 to 1 μm; however, Figure 2d still shows a positive correlation between σ and N. The reason could be that during homogeneous mixing, some droplets completely evaporate, which decreases σ and N at the same time.

[13] More detailed information can be seen in Figure 3, which shows the cloud droplet size distributions color coded by their respective λ values. It is evident that a larger λ corresponds to an increase in small droplets and a decrease in big droplets, affirming the dominance of homogeneous mixing. This dominance may be an important reason why none of the cumulus clouds studied was drizzling.

4. Further Examination

[14] The above analyses suggest that the RACORO cumulus clouds were predominantly affected by homogeneous mixing processes. Recently, *Lu et al.* [2013b] introduced and examined three measures of homogeneous mixing degree based on the relationship between r_v^3/r_{va}^3 and N/N_a, where r_{va} and N_a are the adiabatic volume mean radius and number concentration, respectively. They found that the three measures were similar in terms of their relationships with a dynamic measure of entrainment mixing mechanisms, transition scale number ([*Lu et al.*, 2011], and see Auxiliary Material for its definition). One measure of homogeneous mixing degree stood out as having the tightest relationship with the transition scale number. Here we examine the behavior of this homogeneous mixing degree to further affirm quantitatively the conclusion that the clouds are predominantly affected by homogeneous mixing processes.

[15] The measure of homogeneous mixing degree (ψ) is redefined in Figure 4. State 1 represents an adiabatic cloud. State 2 is the cloud state just after entrainment but before evaporation. From States 2 to 3, mixing and evaporation

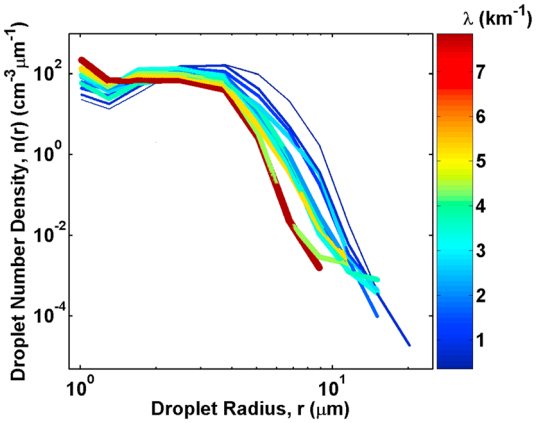

Figure 3. Cloud droplet size distributions as a function of entrainment rate (λ) in 186 growing cumulus clouds during RACORO. The entrained dry air is assumed to be from D to $2D$ away (horizontally) from the edge of cloud core, where here $D = 50$ m.

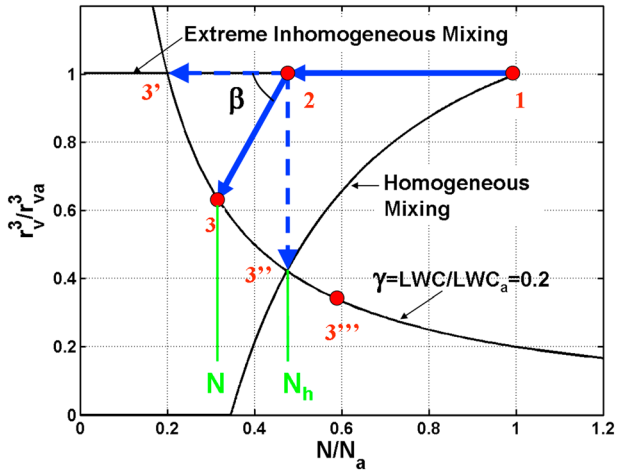

Figure 4. Diagram illustrating the definition of the homogeneous mixing degree. The three black solid lines correspond to extreme inhomogeneous mixing, homogeneous mixing (relative humidity of the dry air is 66%), and the contour of $\gamma = 0.2$, where γ is the ratio of liquid water content (LWC) to its adiabatic value (LWC_a).

occur (see more explanation on these states in the work of *Lu et al.* [2013b]). State 3 is located along the contour of LWC/LWC_a but cannot go beyond the homogeneous mixing line; i.e., N has to be smaller than the number concentration during homogeneous mixing (N_h). However, when analyzing cloud observational data, State 3 may go beyond the homogeneous mixing line (e.g., State 3'''), which could be due to secondary reactivation in clouds or possibly due to the uncertainty of N_a. In the definition of ψ by *Lu et al.* [2013b], State 3''' was not accounted for and ψ was defined as follows:

$$\psi = \frac{\beta}{\pi/2} \tag{2a}$$

$$\beta = \tan^{-1}\left(\frac{\frac{r_v^3}{r_{va}^3} - 1}{\frac{N}{N_a} - \frac{N_h}{N_a}}\right) \tag{2b}$$

where β is the angle between the line linking States 2 and 3 and the line for extreme inhomogeneous mixing and $\pi/2$ is the angle between the line linking States 2 and 3" and the line for extreme inhomogeneous mixing. In this case, $\beta < \pi/2$ and $N < N_h$. To account for State 3''', where $\beta \geq \pi/2$ and $N \geq N_h$, β is redefined as follows:

$$\beta = \tan^{-1}\left(\frac{\frac{r_v^3}{r_{va}^3} - 1}{\frac{N}{N_a} - \frac{N_h}{N_a}}\right) \text{ for } N < N_h \tag{3a}$$

or

$$\beta = \pi + \tan^{-1}\left(\frac{\frac{r_v^3}{r_{va}^3} - 1}{\frac{N}{N_a} - \frac{N_h}{N_a}}\right) \text{ for } N \geq N_h \tag{3b}$$

[16] First, we examine ψ for the average status of the 186 cumulus cloud cores to quantitatively examine the entrainment mixing mechanism that was qualitatively discussed above with Figures 1–3. The average LWC_a in the 186 cumulus cloud cores is 0.298 g m^{-3}. The average N_a is 1107 cm^{-3}, which is the average value of the maximum number concentration in each of the cloud cores. With LWC_a and N_a, r_{va} can be calculated by

$$r_{va} = \left(\frac{LWC_a}{4/3\pi\rho N_a}\right)^{1/3} \tag{4}$$

[17] The average r_v and N of the cloud cores are 3.44 μm and 847 cm^{-3}, respectively. The average N_h is $N_a \times \chi$, and the average χ changes from 0.78 to 0.90 as D increases from 10 to 500 m. Calculation with the above quantities shows that ψ varies from 98% to 78% as D increases from 10 to 500 m. According to *Lu et al.* [2012a], the dry air sources for D varying between 10 and 500 m most likely represent all possible dry air sources in the lateral mixing processes (i.e., air close to and remote from the cloud core); thus, ψ for all possible dry air sources should be within the range of 78% to 98%, suggesting the dominance of homogeneous mixing in the RACORO shallow cumulus clouds.

[18] Second, to examine the entrainment mixing mechanism in individual clouds, ψ is calculated for each cloud core. Figure S6 shows the occurrence frequency of ψ for the 186 cloud cores for different D values (see Auxiliary Material for details). Among the 186 clouds, the number of clouds with ψ >50% varies from 173 to 145 as D increases from 10 to 500 m. Therefore, homogeneous mixing also dominates in individual clouds. Some clouds have ψ values >100% and go beyond the homogeneous mixing line in Figure 4. As mentioned above, this could be attributed to secondary reactivation in clouds or possibly the uncertainty in N_a. All the droplet size distributions in Figure 3 have peaks around 1 μm, which may be partly caused by secondary reactivation. Similarly to LWC_a, N_a is obtained from N averaged over 5 m and N_a could be larger if the averaging distance was smaller. In addition, *Freud et al.* [2011] pointed out that N_a determined from the observed maximum number concentration may be sensitive to small-scale processes and may be affected by the extent of dilution that the cloud has experienced. For each D, only one cloud has ψ <0, i.e., a positive numerator ($\frac{r_v^3}{r_{va}^3} - 1$) and a negative denominator ($\frac{N}{N_a} - \frac{N_h}{N_a}$) in equation (3a). The positive numerator ($\frac{r_v^3}{r_{va}^3} - 1$) indicates $r_v > r_{va}$; thus, the cloud droplets are subjected to superadiabatic growth during inhomogeneous mixing with subsequent ascent in this cloud [*Lu et al.*, 2013a].

5. Concluding Remarks

[19] The relationships between entrainment rate and microphysics are investigated using the data collected from shallow cumuli during the RACORO field campaign. It is found that entrainment rate is negatively correlated with liquid water content, number concentration, standard deviation, mean radius, and volume mean radius but positively correlated with relative dispersion (the ratio of standard deviation to mean radius). These relationships are consistent with the dominance of homogeneous mixing processes in the clouds. The positive correlation between entrainment rate and relative dispersion and the negative correlation between entrainment rate and droplet size suggest that entrainment causes a broadening of droplet size distributions toward smaller sizes, which is unfavorable to warm rain initiation in the cumulus clouds examined.

[20] The dominance of the homogeneous mixing mechanism is qualitatively confirmed by the positive correlations of volume mean radius with number concentration and with liquid water content and by the effects of entrainment rate on cloud droplet size distributions. It is also quantitatively verified using homogeneous mixing degree, which is a quantity defined by *Lu et al*. [2013b] and modified here. The homogeneous mixing degree calculated using the average properties in the 186 cumulus clouds is greater than 78%. When this quantity is calculated for each of the 186 cumulus clouds, the number of clouds mainly affected by homogeneous mixing varies from 173 to 145 as D increases from 10 to 500 m; D represents the distance from the cloud core edge where the mixing dry air originates. The dominance of homogeneous mixing could partially account for why none of the cumulus clouds studied was drizzling.

[21] Three points are worth noting. First, the conclusion of homogeneous mixing dominance in this study holds only for the cumulus clouds examined here. Some previous studies have also shown that inhomogeneous mixing is the dominant mechanism [*Gerber et al*., 2008; *Lu et al*., 2011]. We plan to extend this study to clouds affected mainly by inhomogeneous mixing. Second, *Pawlowska et al*. [2006] analyzed the standard deviation, mean radius, and relative dispersion in marine stratocumulus clouds and pointed out that it was reasonable to assume a constant standard deviation (in the range of 1 to 2 μm) in the parameterization of relative dispersion. Based on the results here, it is still reasonable to assume a constant standard deviation, but in the range of 0.75 to 1 μm for cumulus clouds. Third, the estimation of entrainment rate is based on observations at one aircraft penetration level in each cloud. The accuracy of estimated entrainment rate would be improved if observations at more levels in each cloud were available.

[22] **Acknowledgments.** This research was supported by open funding from the Key Laboratory for Aerosol-Cloud-Precipitation of China Meteorological Administration (no. KDW1201), Nanjing University of Information Science and Technology, China, and Scientific Research Foundation (2012X041), Nanjing University of Information Science and Technology (C. Lu); by the Qing-Lan Project for Cloud-Fog-Precipitation-Aerosol Study in Jiangsu Province, China, a project funded by the Priority Academic Program Development of Jiangsu Higher Education Institutions (C. Lu and S. Niu); and by the U.S. Department of Energy (DOE) Earth System Modeling (ESM) program via the FASTER project (www.bnl.gov/esm) and Atmospheric System Research (ASR) program (C. Lu, Y. Liu, and A. M. Vogelmann). We appreciate the helpful discussions about the RACORO data with Haf Jonsson, Greg McFarquhar, Glenn Diskin, Gunnar Senum, and Hee-Jung Yang.

References

Baker, M. B., R. G. Corbin, and J. Latham (1980), The influence of entrainment on the evolution of cloud droplet spectra: I. A model of inhomogeneous mixing, *Q. J. R. Meteor. Soc.*, *106*(449), 581–598, doi:10.1002/qj.49710644914.

Clothiaux, E. E., T. P. Ackerman, G. G. Mace, K. P. Moran, R. T. Marchand, M. A. Miller, and B. E. Martner (2000), Objective determination of cloud heights and Radar reflectivities using a combination of active remote sensors at the ARM CART sites, *J. Appl. Meteorol.*, *39*(5), 645–665.

Deng, Z., C. Zhao, Q. Zhang, M. Huang, and X. Ma (2009), Statistical analysis of microphysical properties and the parameterization of effective radius of warm clouds in Beijing area, *Atmos. Res.*, *93*(4), 888–896, doi:10.1016/j.atmosres.2009.04.011.

Diskin, G. S., J. R. Podolske, G. W. Sachse, and T. A. Slate (2002), Open-path airborne tunable diode laser hygrometer, *Proc. SPIE*, *4817*, 196–204.

Freud, E., D. Rosenfeld, and J. R. Kulkarni (2011), Resolving both entrainment mixing and number of activated CCN in deep convective clouds, *Atmos. Chem. Phys.*, *11*(24), 12887–12900.

Gerber, H. E., G. M. Frick, J. B. Jensen, and J. G. Hudson (2008), Entrainment, mixing, and microphysics in trade-wind cumulus, *J. Meteorol. Soc. Jpn.*, *86A*, 87–106.

Hill, A. A., G. Feingold, and H. Jiang (2009), The influence of entrainment and mixing assumption on aerosol-cloud interactions in marine stratocumulus, *J. Atmos. Sci.*, *66*(5), 1450–1464.

Jensen, J. B., P. H. Austin, M. B. Baker, and A. M. Blyth (1985), Turbulent mixing, spectral evolution and dynamics in a warm cumulus cloud, *J. Atmos. Sci.*, *42*(2), 173–192, doi:10.1175/1520-0469(1985)042<0173:TMSEAD>2.0.CO;2.

Lasher-Trapp, S. G., W. A. Cooper, and A. M. Blyth (2005), Broadening of droplet size distributions from entrainment and mixing in a cumulus cloud, *Q. J. R. Meteor. Soc.*, *131*(605), 195–220, doi:10.1256/qj.03.199.

Lehmann, K., H. Siebert, and R. A. Shaw (2009), Homogeneous and inhomogeneous mixing in cumulus clouds: dependence on local turbulence structure, *J. Atmos. Sci.*, *66*, 3641–3659, doi:10.1175/2009JAS3012.1.

Lu, C., Y. Liu, and S. Niu (2011), Examination of turbulent entrainment-mixing mechanisms using a combined approach, *J. Geophys. Res.*, *116*, D20207, doi:10.1029/2011JD015944.

Lu, C., Y. Liu, S. Niu, and A. M. Vogelmann (2012a), Lateral entrainment rate in shallow cumuli: Dependence on dry air sources and probability density functions, *Geophys. Res. Lett.*, *39*(20), L20812, doi:10.1029/2012GL053646.

Lu, C., Y. Liu, S. S. Yum, S. Niu, and S. Endo (2012b), A new approach for estimating entrainment rate in cumulus clouds, *Geophys. Res. Lett.*, *39*, L04802, doi:10.1029/2011GL050546.

Lu, C., Y. Liu, and S. Niu (2013a), A method for distinguishing and linking turbulent entrainment mixing and collision-coalescence in stratocumulus clouds, *Chi. Sci. Bull.*, *58*, 545–551, doi:10.1007/s11434-012-5556-6.

Lu, C., Y. Liu, S. Niu, S. K. Krueger, and T. Wagner (2013b), Exploring parameterization for turbulent entrainment-mixing processes in clouds, *J. Geophys. Res.*, *118*, 185-194, doi:10.1029/2012JD018464.

Pawlowska, H., W. W. Grabowski, and J. L. Brenguier (2006), Observations of the width of cloud droplet spectra in stratocumulus, *Geophys. Res. Lett.*, *33*(L19810), L19810, doi:10.1029/2006GL026841.

Romps, D. M. (2010), A direct measure of entrainment, *J. Atmos. Sci.*, *67*(6), 1908–1927, doi:10.1175/2010JAS3371.1.

Sanderson, B., C. Piani, W. J. Ingram, D. A. Stone, and M. R. Allen (2008), Towards constraining climate sensitivity by linear analysis of feedback patterns in thousands of perturbed-physics GCM simulations, *Clim. Dyn.*, *30*(2-3), 175–190.

Stommel, H. (1947), Entrainment of air into a cumulus cloud, *J. Meteorol.*, *4*(3), 91–94, doi:10.1175/1520-0469(1947)004<0091:EOAIAC>2.0.CO;2.

Su, C.-W., S. K. Krueger, P. A. McMurtry, and P. H. Austin (1998), Linear eddy modeling of droplet spectral evolution during entrainment and mixing in cumulus clouds, *Atmos. Res.*, *47-48*, 41–58.

Vogelmann, A. M., et al. (2012), RACORO extended-term aircraft observations of boundary layer clouds, *Bull. Am. Meteorol. Soc.*, *93*(6), 861–878, doi:10.1175/bams-d-11-00189.1.